8

Bioradiolocation as a Technique for Remote Monitoring of Vital Signs

Lesya Anishchenko, Timothy Bechtel, Sergey Ivashov, Maksim Alekhin, Alexander Tataraidze, and Igor Vasiliev

CONTENTS

8.1 Introduction

8.1.1 Chapter Overview

This chapter summarizes the results of investigations into the applications of radar in medicine. Bioradars provide a wide range of possibilities for remote and noncontact monitoring of the psycho-emotional state and physiological condition of many macro-organisms. In particular, this chapter provides information on the technical characteristics of bioradars designed at Bauman Moscow State Technical University (BMSTU), Russia, in international collaboration with Franklin & Marshall College, Lancaster, PA, and on experiments using these radars. The results of experiments demonstrate that bioradars of BioRASCAN type may be used for simultaneous remote measurements of respiration and cardiac rhythm parameters. In addition, bioradar-assisted experiments for detection of various sleep disorders are described. The results prove that bioradiolocation allows accurate diagnosis and estimation of obstructive sleep apnea severity, and could be used in place of polysomnography, which is considered the current standard medical evaluation method, but requires direct patient contact.

8.1.2 Bioradiolocation Fundamentals and Applications

Bioradiolocation (BRL) is a modern sensing technique that provides the capability to detect and monitor persons remotely (even when behind optically opaque obstacles) without applying any contact sensors. It is based on reflected radar signal modulation by oscillatory movements of human limbs and organs. Electromagnetic waves reflected from the human body contain specific biometric modulations, which are not present when the waves interact with motionless objects. The main contributors to these signals are heartbeat; contractions of vessels; gross movements of limbs; and the reciprocal movements of the chest wall and abdomen associated with breathing. Thus, a patient's or subject's physical activity and medical (as well as psychological) state determine the characteristics of these signal fluctuations.

Bioradiolocation has a variety of potential application areas in military, law enforcement, medicine, etc. A detailed list of these areas is given as follows.

- *Antagonist and hostage localization inside buildings during counter-terrorism operations*: There are a few commercially available bioradars for this application; however, these devices have several limitations, which have not yet been overcome, the most serious of which is high attenuation of bioradar signal when propagating through damp or reinforced concrete walls (Greneker 1997, Droitcour 2001).
- *Disaster response:* Bioradars are used for detection of survivors beneath debris after natural or technological disasters (Chen 2000, Bimpas 2004). The most serious challenge lies in multipath propagation of bioradar signal in rubble, which may contain reflectors at all angles. In addition, reduction in false alarms currently requires cessation of all dismantling activities during the period of scanning with bioradar. Similar techniques may be applied during fire emergency searches (Chen 1986). Chapter 7 discusses signal design for biolocation systems.
- *Battlefield or disaster zone triage*: The application of bioradar could help in remotely distinguishing between wounded and dead casualties and thus establish the order of evacuation and treatment priority (Boric-Lubecke 2008).

- *Transportation safety and security*: Examination of transport containers for detecting stowaways, fugitives, or espionage agents at border crossings or other transit terminals (Greneker 1997).
- *Remote diagnostics of psycho-emotional state*: Screening for undue agitation or anxiety during latent or open screening in criminal investigations or at checkpoints (Greneker 1997).
- *Remote speech detection*: Microwave "eavesdropping" to detect speech and speech patterns if not actual transcription of dialogue (Holzrichter 1998).
- *Contactless registration of respiration and cardiac rhythm*: Important for, e.g., burn patients and others for whom contact sensors cannot be applied (Greneker 1997, Droitcour 2001, Staderini 2002).
- *Sleep medicine*: Bioradars can be used to monitor respiration and heartbeat patterns for diagnosis of sleep apnea syndrome (Kelly 2012). In the case of newborns, it is possible to use this method for detection of imminent Sudden Infant Death Syndrom (Li 2010), allowing real-time, immediate, and potentially life-saving response.
- *Estimation of vessel elasticity*: The radar pulse velocity in vessel tissue can reveal patients predisposed to cardiovascular disease (Immoreev 2010).
- *Smart homes*: It is possible to use bioradars to monitoring movements and activities of elderly or invalid subjects in their homes (Li 2010).
- *Tumor tracking*: The size and condition of tumors can be characterized, e.g., during radiation therapy (Li 2010).
- *Laboratory animal locomotor activity monitoring*: Just as for smart homes, the living quarters of valuable lab animals can be monitored remotely without disturbing them (Anishchenko 2009).

In practice, there are several challenges in achieving reliable registration of respiration and heart rate parameters using bioradar. Among them are: clutter caused by surrounding objects and multipath propagation, artifacts from gross body movements with amplitude much bigger than the desired signals, and problems with isolation and discrimination of respiration and heartbeat signals during prolonged monitoring. These challenges require development of adaptive algorithms for effective extraction of the informative components of bioradar signals, as well as implementation of numerical procedures aimed at improving the accuracy and stability of estimates of physiological parameters such as respiration and heart rate. For example, by applying low-cut filters to reject all near-zero frequencies from the reflected bioradar signal, it is possible to suppress clutter caused by local inanimate objects (Bugaev 2005).

Among the signals suitable for detecting the characteristic signatures of living objects are continuously modulated or nonmodulated microwave signals at frequencies ranging from hundreds of MegaHertz (MHz) to tens of GigaHertz (GHz); narrowband, wideband, or ultrawideband (UWB) signals with appropriate center frequencies; and "noise" pulse signals that have no clearly defined carrier frequency (Immoreev 2010, Li 2012, Wang 2013, Otsu 2011, Ivashov 2004).

The material in this chapter is structured as follows: following the introduction in Section 8.1, Section 8.2 reviews the theory of vital signs registration by means of bioradar using the example of a nonmodulated probing signal. This section will also present two types of processing for separation of co-registered respiratory and heart beat signals. Section 8.3 contains information on methods for verification of the vital signs data recorded by bioradar. Section 8.4 reviews the results of various biomedical experiments using bioradar.

8.2 Bioradiolocation Signal-Processing Methods for Life Signs Monitoring

The presence of biometric information in reflected microwave signals is related to the contraction of the heart, blood vessels, lungs, and other internal organs, as well as movements of the skin surface due to respiration and cardiac pulse. These phenomena are periodic with frequency ranges of approximately 0.8–2.5 Hz for pulse and 0.2–0.5 Hz for respiration. A reflected microwave signal that contains such biometric information is referred to as a biometric radar signal. The useful component of biometric information (related to physiological signatures) is recorded in the parameters of modulation of the biometric radar signal in the time domain as well as in their spectra in the frequency domain. As a result of cyclical recurrence of phenomena related to respiration and pulse, there are corresponding components in the spectrum of a biometric radar signal. The frequencies and amplitudes of these radar signal components roughly match the frequencies and intensities of the breathing and heart beat phenomena. As described below, the theoretical estimation of the spectrum of a reflected signal output from the microwave receiver is of special interest in many applied studies.

8.2.1 Monochromatic Bioradar Signal Processing

8.2.1.1 Theoretical Model of Monochromatic Bioradar Signal

The simplest microwave device capable of recording biometric signatures is a radar with a nonmodulated probing signal described by:

$$\dot{u}_0(t) = U_0 e^{j\omega_0 t} \tag{8.1}$$

Dominant reflections arise at the air–skin interface. The effective area of reflection and therefore area of relevant fluctuations of the skin is located within the limits of one Fresnel zone, with radius r_0. The radius of the effective area of reflection can be written as:

$$r(t) = r_0 + \Delta r(t), \tag{8.2}$$

where D$r(t)$ is characteristic of the fluctuations of the skin. Based on Equation 8.2, the useful signal recorded by the radar will be registered with attenuation factor q and phase shift $\varphi(t)=-2kr(t)$:

$$\dot{u}_c(t) = qU_0 e^{j\omega_0 t - j\varphi_0 - j2k\Delta r(t)}, \tag{8.3}$$

where:

$k = 2p/l$ is wave number
l is radiated signal wavelength
$\varphi_0 = 2kr_0$

Usually, at the input of the receiver, along with the useful reflected signal, the so-called penetrating signal of the transmitter also registers:

$$\dot{u}_{inp}(t) = q_p U_0 e^{j\omega_0 t - j\varphi_p} + qU_0 e^{j\omega_0 t - j\varphi_0 - j2k\Delta r(t)} \tag{8.4}$$

where q_p and φ_p are the attenutation factor and phase of the penetrating signal.

Further, and without reducing generality, it is possible to accept zero phase for the penetrating signal, or $\varphi_p = 0$. We can represent fluctuations of the skin due to breathing and heart beat by a biharmonic function:

$$\Delta r(t) = \Delta_1 \sin(\omega_1 t) + \Delta_2 \sin(\omega_2 t + \varphi_2) \tag{8.5}$$

where:
$\omega_1 = 2\pi f_1$
$\omega_2 = 2\pi f_2$
$f_1, f_2, \Delta_1, \Delta_2$ are frequencies and amplitudes of breathing and heart beating
φ_2 is a constant phase

In the microwave radar spectrum, it is possible to apply either of the two types of receiver. There may be a coherent receiver with two quadrature phase detectors, or an amplitude receiver. However, to overcome the loss of the basic frequencies in a received signal spectrum, one should use the principles of quadrature coherent signal processing (Bugaev 2004).

8.2.1.2 Basic Experiments on Noncontact Cardiorespiratory Parameters Registration Using a Monochromatic Bioradar

At BMSTU, the BRL technique has been investigated since 2003. During the first series of experiments, a modified ground-penetrating radar (GPR) of RASCAN type with operating frequency of 1.6 GHz was employed. The experiments addressed radar sounding of human cardiorespiratory parameters through a brick wall, and demonstrated that the task of remote diagnostics of human cardiorespiratory parameters using continuous-wave subsurface radar (Bugaev 2004) is technically feasible. A sketch of the experiment is shown in Figure 8.1.

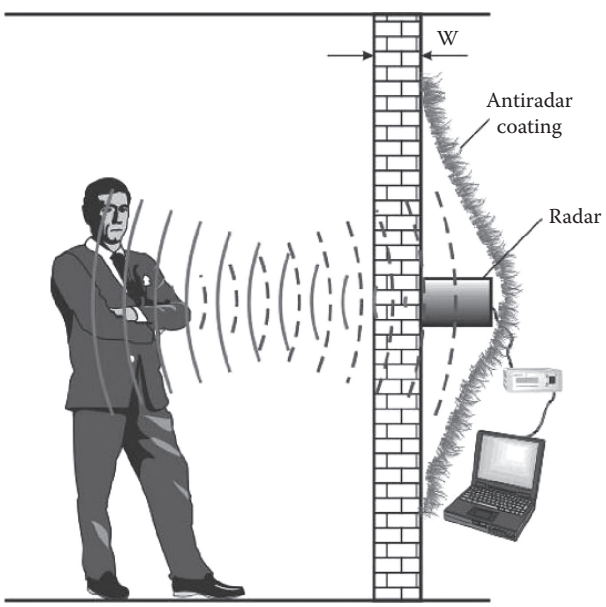

FIGURE 8.1
Sketch of the experiment on through-wall sensing of human cardiorespiratory parameters with a modified ground-penetrating radar ($w = 10$ cm).

The examinee stood behind a 10-cm-thick wall and about 1 m from the wall. The radar antenna was fastened directly at the wall surface. To decrease the interference from reflections of the back lobes of the transmitted signal, the antenna and the part of the wall were veiled by an antiradar (nonreflective) coating with dimensions of 2×2 m.

The reflected radar signals were detected and recorded in the computer memory through an interface module. In Figures 8.2 and 8.3, the pulse record and corresponding signal spectrum for the examinee during a period of breath holding are presented. In Figure 8.2, the breath was held approximately 30 seconds. In Figure 8.3, the hold was about 1 minute. It is clear that with the increase in breath hold time, the amplitude and rate of examinee heartbeat activity are also increased as a result of oxygen deprivation. The results of simultaneous recording of heartbeat and breathing are given in Figure 8.4. The amplitude of breathing oscillations considerably surpasses heart beating vibrations, so a composite response is clearly visible.

The results obtained in the experiments are similar in many respects to the signals registered by time-domain impulse radars in free space (Liu 2012). However, the use of monochromatic wave radars simplifies the experimental installation and subsequent data processing. The experiments on radar sounding of human heartbeat and breathing through a 10-cm-thick brick wall demonstrated that remote diagnostics of human cardiorespiratory parameters using a continuous-wave subsurface radar of RASCAN type is technically feasible.

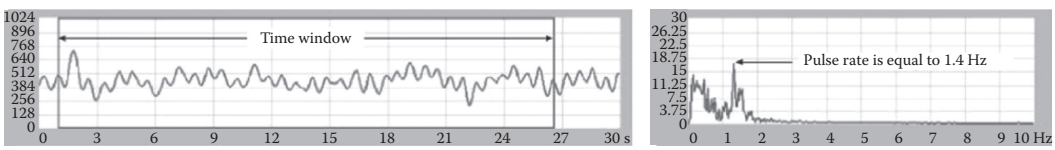

FIGURE 8.2
BRL signal and its spectrum for 30-second breath hold.

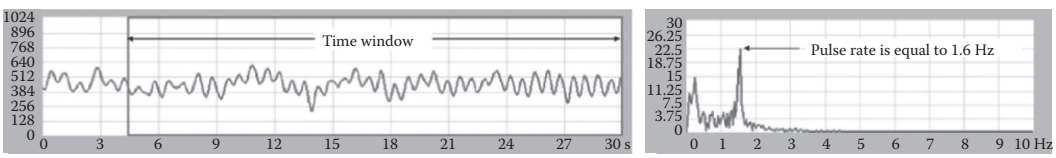

FIGURE 8.3
BRL signal and its spectrum for 60-second breath hold.

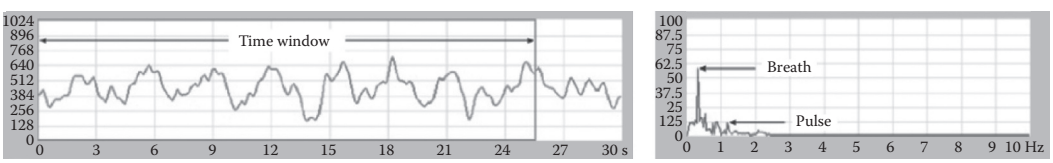

FIGURE 8.4
BRL signal and its spectrum for simultaneous heartbeat and breathing registration.

8.2.2 Comparison of the two Bioradiolocation Signal-Processing Techniques for Noncontact Monitoring of Cardiorespiratory Parameters

Another possible type of bioradar is multifrequency, which allow the estimation of the range to the subject as well as the cardiorespiratory parameters. Using data from this type of bioradar, a feasibility study of life signs detection and characterization using a multifrequency radar system was performed (Soldovieri 2012). The recordings were processed using two different data-processing approaches, with the performance characteristics for each compared in terms of the accuracy of the frequency characterization for respiration and heartbeat.

The BioRASCAN multifrequency bioradar designed at Remote Sensing Laboratory of BMSTU has a quadrature receiver designed to perform remote monitoring of gross human movements, as well as breathing and heartbeat. This radar operates by transmitting and receiving a continuous-wave field in the frequency range from 3.6 GHz to 4.0 GHz. Based on the dielectric constant of air in this waveband, this provides a spatial resolution of approximately 0.5 cm.

The first data processing approach to be considered was previously presented by D'Urso (2009) and was intended to provide frequency analysis of biometric signals by maximizing the scalar product of the Fourier transform of two signals, one representing the measured signal modulated by reflector displacement and the other derived from a theoretical electromagnetic model. The second approach attempted to provide information not only on the frequency of the life signs signals, but also at recovering information on the range of the subject by establishing a range–frequency matrix. Separation of respiration and heartbeat signals was made by the application of rejection filtration to corresponding line of range–frequency matrix (Bugaev 2005, Anishchenko 2008).

Figure 8.5 shows the experiment in which the subject was located in front of the radar system. In particular, the experiment was carried out with a 20-year-old male subject in good health and fitness, and a professional skier. The distance between the antennas and subject was 1 m. The experiment was divided into two stages. During the first stage, monitoring of breathing and pulse parameters at steady state was performed for about 5 minutes. At the second stage, a breath-holding test was performed. It gave a rough index

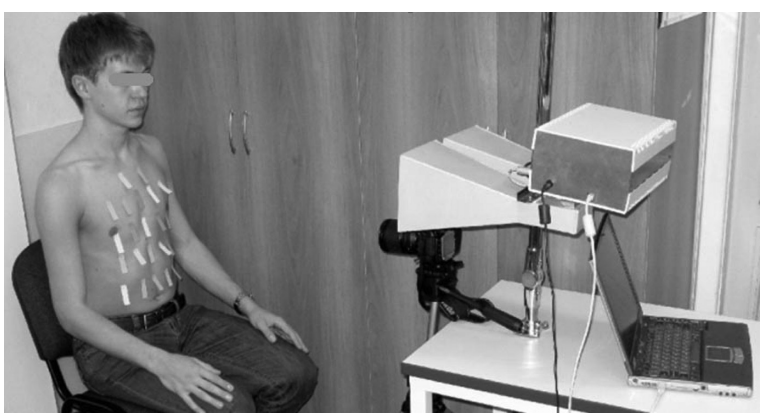

FIGURE 8.5
Photo of the experimental setup.

of cardiopulmonary reserve by measuring the length of time that the subject could hold breath. This is a widely known test in medicine, which is used for estimating physical fitness in the training of pilots, submariners, and divers.

8.2.2.1 The First Bioradiolocation Signal-Processing Approach

As described above, the goal of this test is to detect vital signs (breathing and heartbeat) and to determine their frequency for the case of a human being in free space. This is a simplified model described by Equation 8.5 without the last term corresponding to heartbeat. Computation of the field reflected by the oscillating target exploited quasi-stationarity was done as follows (Soldovieri 2012).

In real conditions, received signal contains clutter (u_{clut}):

$$u_R = U_0 \exp(-2jk(r_0 + \Delta_1 \sin[\omega_1 t])) + u_{clut} \tag{8.6}$$

Thus, the problem at hand is stated as how to estimate the frequency ω_1 starting from the knowledge of the reflected field measured over a finite time interval $[0,T]$.

The proposed reconstruction procedure included the following steps. First was the removal/mitigation of the static clutter, that is, the u_{clut} term in Equation 8.6. The ideal clutter removal strategy would be based on the difference between the actual signal and the one when no vital signs are present (background signal). Since such a background measurement is not available, an alternative strategy is necessary. In this algorithm, the static clutter removal is carried out by the following steps: First, we compute the mean value u_{mean} of the signal over the interval domain; then, we subtract u_{mean} from the measured one $u_R(t)$ to achieve $\tilde{u}_R(t) = u_R(t) - u_{mean}$. The subsequent processing is then performed on $\tilde{u}_R(t)$. Next, Fourier transformation is performed on the resulting signal to compute the function $G(\omega_1)$ in Doppler domain. The Fourier transform of the model signal $\exp(-2jk\Delta_1 \sin(\omega_1 t))$ is computed as:

$$\begin{aligned} u_{\mathrm{mod}\,el}(\omega_1) &= \int_0^T \exp(-2jk\Delta_1 \sin(\omega_1 t)) \exp(-j\omega_1 t) dt = \\ &= \int_0^T \sum_{n=-\infty}^{\infty} J_{-n}(2k\Delta_1) \exp(jn\omega_1 t) \exp(-j\omega_1 t) dt = \\ &= \sum_{n=-\infty}^{\infty} J_{-n}(2k\Delta_1) \sin c\left[\frac{T}{2}(\omega_1 - n\omega_1)\right] \exp\left(-j(\omega_1 - n\omega_1)\frac{T}{2}\right) \end{aligned} \tag{8.7}$$

where we exploit the well-known Fourier expansion of the term $\exp(-2jk\Delta_1 \sin(\omega_1 t))$, and $J_n(\bullet)$ denotes the Bessel function of first kind and nth order. Therefore, the Fourier transform $u_{\mathrm{mod}\,el}(\omega_1)$ is made up of a train of sin$c$ functions centred at $n\omega_1$.

Finally, the unknown Doppler frequency ω_1 is determined as the quantity that maximizes the scalar product between the modulus of the measured Fourier transform $|G(\omega_1)|^2$ and the modulus of the Fourier transform of the model signal $|u_{\mathrm{model}}(\omega_1)|^2$.

It is worth noting that in the above-outlined procedure, the maximum displacement is still unknown. In principle, such a quantity could be determined together with the Doppler frequency to maximize the scalar product. However, in the case at hand, in order to make the determination procedure fast enough for realistic conditions, we assume an estimate of the maximum displacement as $\Delta_1 = 0.5\,\mathrm{cm}$ for the breathing and 1 mm for heartbeat.

8.2.2.2 The Second Bioradiolocation Signal-Processing Approach

The second data-processing approach is designed to gain information not only about the frequency behavior of life signs, but also about the range of the investigated subject (Bugaev 2005, Anishchenko). The steps in this procedure are as follows.

The first step is to build a range–frequency matrix (Bugaev 2005); this matrix contains all possible signal reflections including ones from motionless objects, located in different range cells. These objects are the cause of static clutter. The range–frequency matrix resulting from the suppression of the zero or nearly zero frequencies is given in the upper panel of Figure 8.6.

The separation between the breathing and heartbeat signals is carried out next using rejection of the frequency components corresponding to breathing in the range–frequency matrix, and the result is shown in the lower panel of Figure 8.6.

Reconstruction of breathing and heartbeat signals is carried out by applying inverse an Fourier transform to the matrix row corresponding to the distance to the examinee (1.1 m) and evaluating its phase. Signals obtained in this fashion corresponding to range–frequency matrices from Figure 8.6 are shown in Figure 8.7, which clearly show good performance of this approach in separating breathing and heartbeat signals.

8.2.2.3 Bioradiolocation Signal Reconstruction Results

After separating the signals for breathing and pulse, the reconstruction of these signals is necessary. It can be made at any of the probing frequencies. Figures 8.8 and 8.9 compare the reconstructed signals for respiration and pulse at the 3.6 GHz probing frequency.

For better performance, the recorded bioradar signal was divided into 19 time windows, each consisting of 1024 time samples (for a time interval length of 16.3 seconds). For each of these intervals, the two data-processing approaches described above were applied.

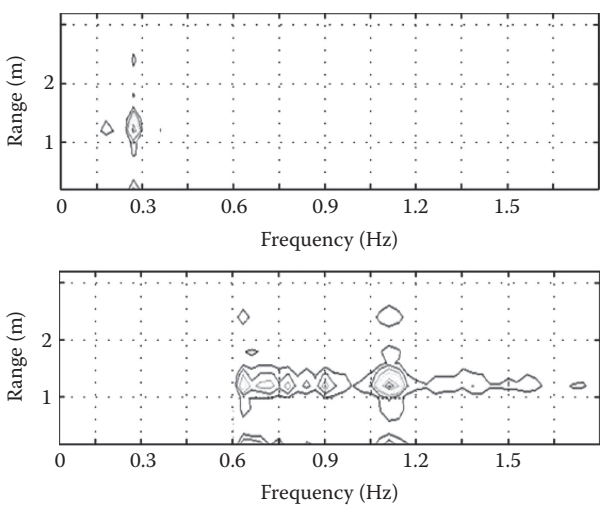

FIGURE 8.6
Range–frequency matrix for the examinee at 1.1 m range: (a) (upper) before breathing harmonics rejection; (b) (lower) after breathing harmonics rejection.

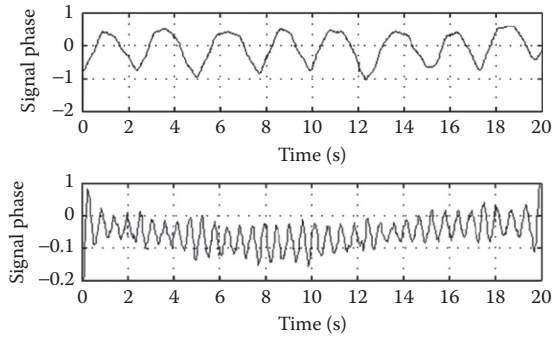

FIGURE 8.7
Reconstructed breathing (a) and heartbeat (b) signals of the subject corresponding to the range–frequency matrices from Figure 8.6 (the signal phase is normalized with respect to its maximum).

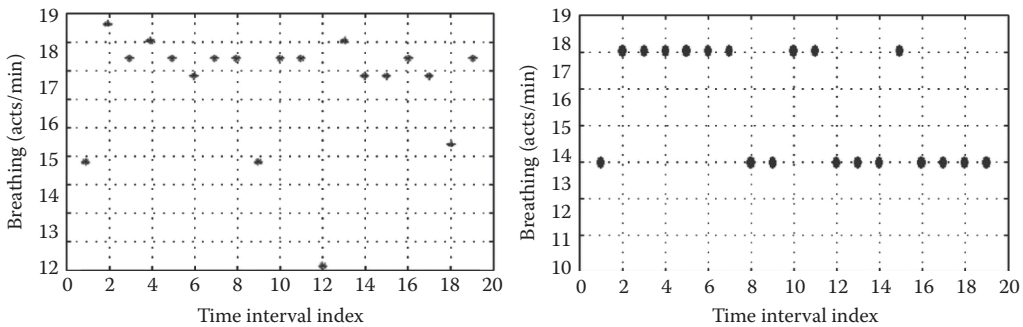

FIGURE 8.8
Comparison between the data processing approaches for respiration monitoring. (a) first data processing approach; (b) second data processing approach.

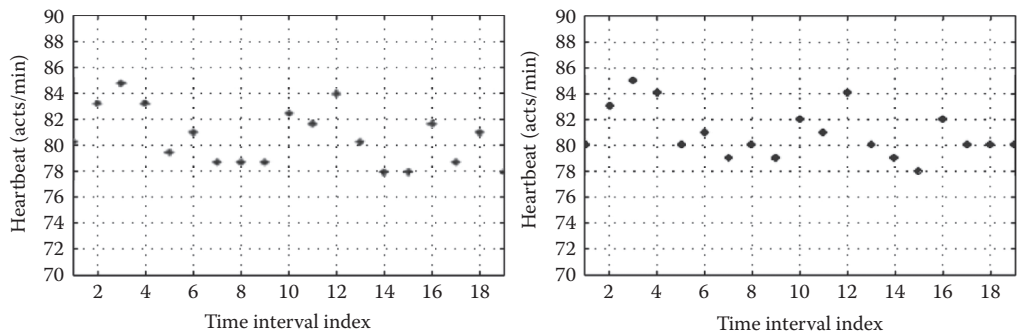

FIGURE 8.9
Comparison between the data processing approaches for pulse monitoring. (a) first data processing approach; (b) second data processing approach.

In both the respiration and pulse recordings, a good agreement is observed between the results for the two data-processing approaches; in particular, an almost uniform breathing behavior is observed with a frequency of 18 beats/min apart from few time intervals.

It can be seen that the average pulse frequency is about 80 beats per minute. In addition, we can note a correlation between the time behavior of the breathing

and the one for heart beat. Specifically, when the breathing frequency decreases, the heartbeat frequency also decreases.

8.3 Verification of Bioradiolocation with Standard Contact Methods

For effective application of any new method in medicine, measured vital signs parameters must be verified using current best-practice or gold-standard methods. For heart beat and breathing frequency estimation, the gold-standard methods are ECG and respiratory impedance plethysmography (RIP), respectively (Konno and Mead, 1967). This section presents the verification testing for BioRASCAN measurements.

8.3.1 Verification of *Bioradiolocation* and ECG

Comparative experiments for BioRASCAN and ECG methods were carried out to confirm that the bioradar can be used for accurate heart rate monitoring as shown in Figure 8.10.

The test population of 52 adult examinees consisted of 23 males and 29 females with a mean age 20 ± 1 years (mean ± SD) participated in the verification experiments. During the experiment, each subject sat in a relaxed pose in front of the bioradar at a distance of 1 m from antennas. For each subject, bioradar and ECG signals were recorded three times for a duration of 1 minute per record. Comparison of the measured heart beat frequency values for both methods were compared, yielding a good agreement with a confidence level of $p = 0.95$. Thus, the feasibility of BRL for simultaneous measurements of breathing and heart rate parameters was demonstrated at a statistically significant level.

8.3.2 Verification of Long Records of Bioradiolocation Signals with Respiratory Plethysmography

Previously, experiments to verify respiratory patterns using BRL were made in idealized conditions with short records, and motionless subjects facing the bioradar atennas (Massagram 2011, Droitcour 2009, Vasu 2011, Alekhin 2013). In this section, we present

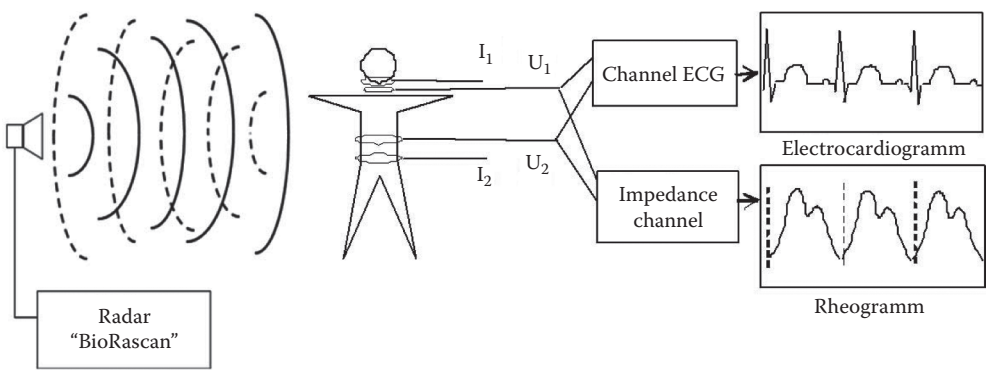

FIGURE 8.10
Sketch of the experiment to verify BioRascan measurements against conventional measurements.

FIGURE 8.11
Photos of the experiment comparing simultaneous registration of BRL (radar) and conventional polysomnography (PSG) data.

experimental results obtained in close-to-real conditions (during a full night of sleep) during which examinees could change their position and move their limbs freely.

Five subjects without sleep breathing disorders underwent sleep study at the Sleep Laboratory of the Federal Almazov Medical Research Centre (Saint Petersburg, Russia). During the experiment, BRL and RIP signals were registered simultaneously throughout a night of sleep as shown in Figure 8.11. Full-night polysomnography (PSG) using an Embla N7000 by Embla Systems LLC, Ontario, Canada, was performed, including registration of respiratory movements by RIP. BRL monitoring was done using a BioRASCAN with operating frequency band 3.6–4.0 GHz.

Detection of inhalation peaks based on BRL and RIP signals was performed. A data-processing algorithm was used for the RIP signal inspiratory peaks detection, consisting of the following steps: summation (half of sum of the abdominal and thoracic RIP signals was used in the subsequent analysis); filtration (3rd-order Butterworth filter operating in 0.2–1.0 Hz frequency range was applied); and detection (inspiratory peaks were detected by an algorithm to find local maxima). The BRL signal shown in Figure 8.12 compared with the RIP signal had the following peculiarities: subjects' movements make more artifacts; there are strong amplitude changes resulting from the subjects' full body displacement; phase shifts result from flip-over signals, making inspiratory peaks downward.

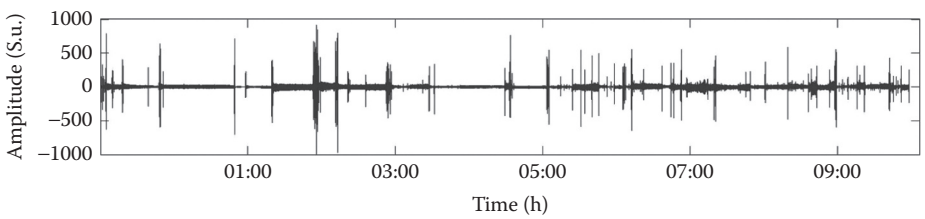

FIGURE 8.12
Original BRL signal recorded prior to signal-processing stage.

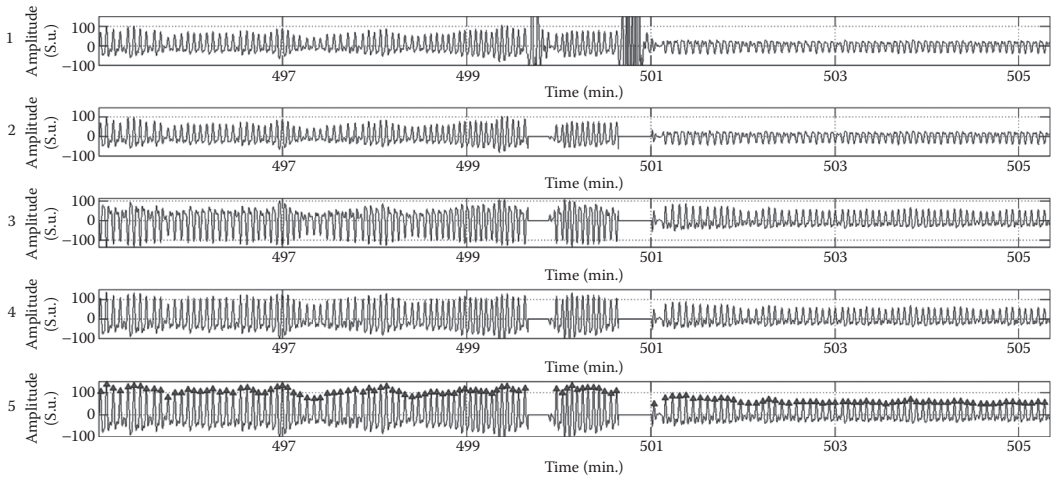

FIGURE 8.13
Results of the inspiratory peak detection algorithm steps: 1 – filtered signal; 2 – signal after movement artifact rejection; 3– combined signal comprising the best interartifacts parts of signals; 4 – signal after phase shift rejection; 5 - inspiratory peak detection.

The results of BRL signal processing at different steps in the inspiratory peak detection algorithm are given in Figure 8.13.

For the comparison/verification, the start of the BRL and RIP signals were peak-to-peak synchronized. BRL and RIP signals were truncated to the sleep period, i.e., parts of the signals recorded during waking before and after sleep intervals were deleted. Intervals of RIP signal corresponding to intervals of BRL signal marked as artifacts were also rejected. Inspiratory peak counts per minute (respiratory rhythm) were calculated for the RIP and BRL signals shown in Figure 8.14. Further, Pearson's correlation coefficient was calculated between respiratory rhythms obtained by RIP and BRL methods for each subject.

Although RIP and BRL signals were initially peak-to-peak synchronized, they subsequently desynchronized as shown in Figure 8.15. Since desynchronization is not more than a half of respiratory cycle, this is not a problem, and is apparently due to the absence of continuous or periodic time synchronization between the BioRASCAN and Embla devices.

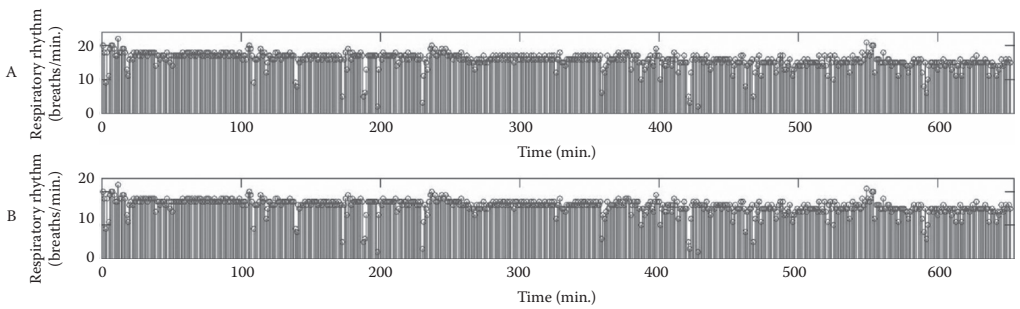

FIGURE 8.14
Comparison of respiratory rhythm estimation by BRL (A) and RIP (B) signals.

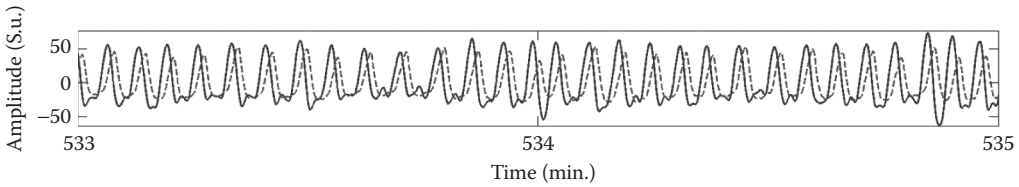

FIGURE 8.15
BRL and RIP signal desynchronization (the solid plot is the BRL signal; the dashed line is the RIP signal).

The cross-correlation coefficient for BRL and RIP results of 0.97 indicates a very strong correlation. The artifact time mean value of 6.8% shows high sensitivity of BRL to movements. Although a small number of subjects were tested, these results proved that bioradars may be used for accurate noncontact monitoring of breathing patterns during prolonged periods, e.g., in sleep studies.

8.4 Experimental Study on Prospective Applications of Bioradiolocation Technology in Biomedical Practice

This section reviews the bioradar-assisted experiments, which were carried out at BMSTU since 2006. Two bioradars BioRASCAN-4 and BioRASCAN-14 operating in different frequency ranges were used for conducting the experiments. Table 1 presents their technical characteristics (Table 8.1).

8.4.1 Automated *Estimation* of *Sleep Quality* during *Prolonged Isolation*

One of the most promising areas of bioradar application in medicine is somnology (the scientific study of sleep). In 2009, BMSTU conducted the first experiment to investigate the possibility of bioradar usage for noncontact sleep quality estimation. Bioradar signals were recorded during an entire night of sleep for the examinee. Six overnight records were made for a heatly adult male (aged 20 years).

Processing of the recorded signals was performed in stages using MATLAB. First to eliminate baseline drift, the bioradar signal was filtered using the built-in MATLAB

TABLE 8.1
Technical characteristics of BioRASCAN radars

	BioRASCAN-4	BioRASCAN-14
Number of frequencies	16	
Operating frequency band, GHz	3.6–4.0	13.6–14.0
RF output, mW	<3	
Gain constant, dB	20	
Detecting signals band, Hz	0.03–5.00	0.03–10.00
Dynamic range of the detecting signals, dB	60	
Size of antenna block, mm	370×150×150	120×50×50
Sensitivity, mm	1.0	0.1

Butterworth digital filter with cutoff frequency of 0.05 Hz (filter order of 8). Then, intervals of movement activity were detected. It is obvious that the level of the received signal, which corresponds to calm breathing and whole body movement, differs by more than a factor of 10 in amplitude. However, the main problem in detecting movement artifacts is the fact that the examinee may turn from one side to other during sleep. In this case, the distance between antenna and examinee and the scattering cross section of the target may change. As a result, the level of the received bioradar signal may also vary significantly before and after movement artifact as shown in Figure 8.16.a.

That is why it is not enough to use only signal amplitude parameters for the detection of movement episodes. However, episodes during which movement signal artifacts are present contain higher frequency components (greater than 1 Hz) than during times of regular breathing (0.1 to 0.6 Hz). These spectral differences were used in the algorithm for movement artifact detection.

Respiration frequency is estimated only for intervals free from movement artifacts and shown in Figure 8.17. The mean values for breathing intervals were calculated for every 30 seconds as it is usually done while processing somnology data (Rechtschaffen 1968).

Due to the successful results of the studies described above, bioradar experiments were included in the scientific program of the international research project MARS-500 (simulation of prolonged isolation during a manned flight to Mars), which was led by the Institute for Biomedical Problems Russian Academy of Science from June 2010 to November 2011.

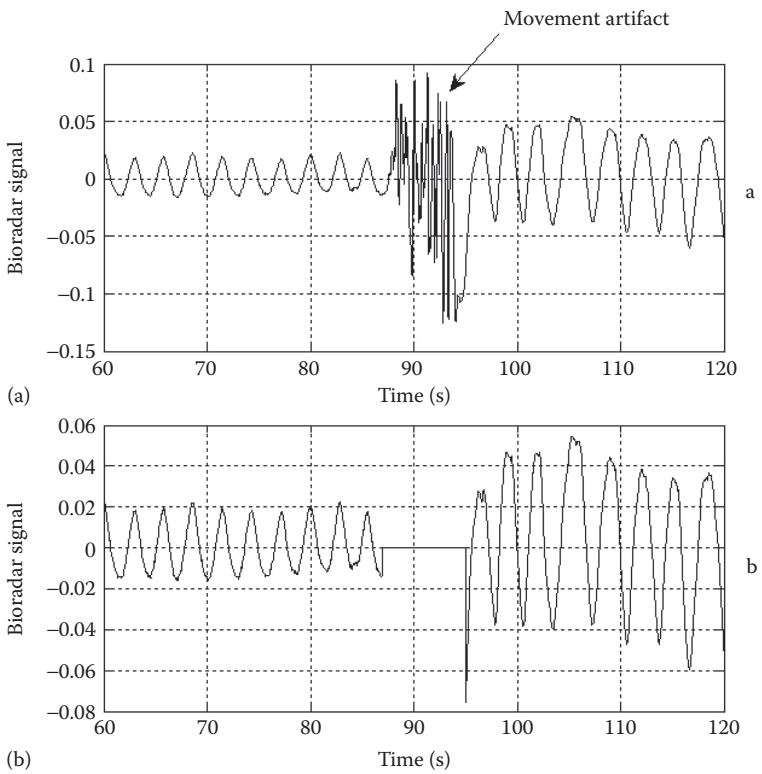

FIGURE 8.16
Bioradar signal before (a) and after (b) movement artifact extraction.

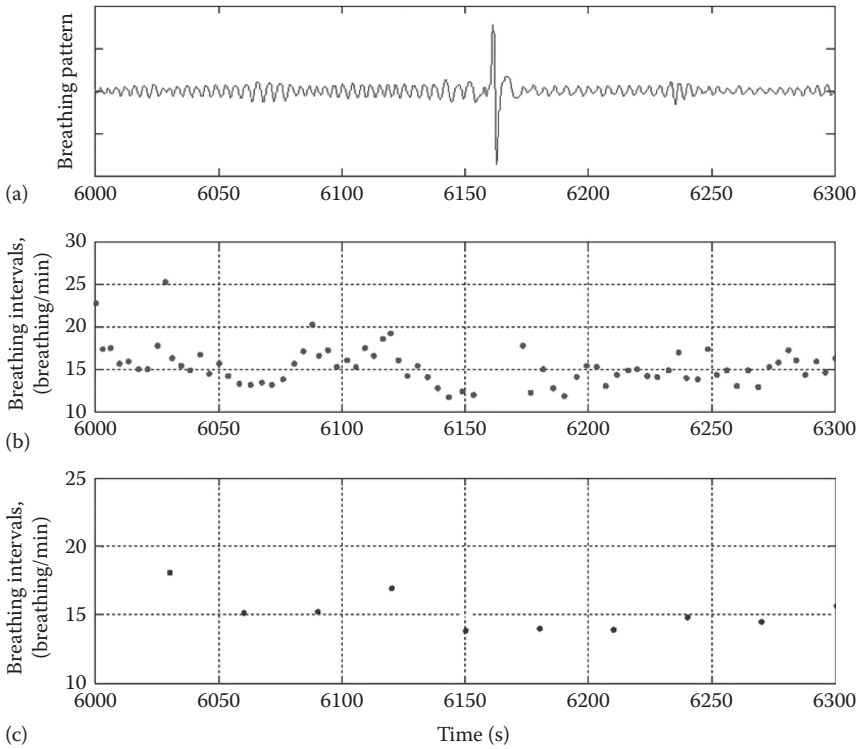

FIGURE 8.17
Example bioradiolocation signals from trials on patients with and without diagnosed sleep disorders. Top: patient with Central Sleep Apnea (CSA), Middle: Obstructive Sleep Apnea (OSA), Bottom: Normal Calm Sleeping (NCS).

Due to the prolonged isolation, an ethical committee approval and informed consent from all MARS-500 crewmembers was obtained before the start of the experiment. The crew was trained to conduct their own bioradar experiments. During the project, seven series of bioradar experiments were conducted for each of six crew members. As it turned out, it was more convenient to use hourly averages of parameters to record their dynamic ranges during a full night of sleep. The results of the experimental data recorded for one of the MARS-500 crew members are given in Figure 8.18.

It is known that the breathing pattern and movement activity dynamics are characteristic of individuals, and do not usually change greatly from night to night. If changes take place, it may indicate that the examinee suffers from some kind of stress during day time. Using the proposed algorithm, it is possible to monitor breathing and movement activity pattern and thus detect a sleep disturbance caused by daytime stress. In Figure 8.18, the changes in breathing frequency dynamics along the duration of the project for one of the crewmembers are presented. It is clearly seen that for the first half of the experiment (from June 2010 through January 2011) after falling asleep, the respiration frequency of the examinee decreased, but during the last hour of sleep, breathing frequency became higher. However, for the second half of the experiment (from January 2011 through July 2011), the breathing pattern during sleep changed, perhaps indicating stress caused by prolonged isolation.

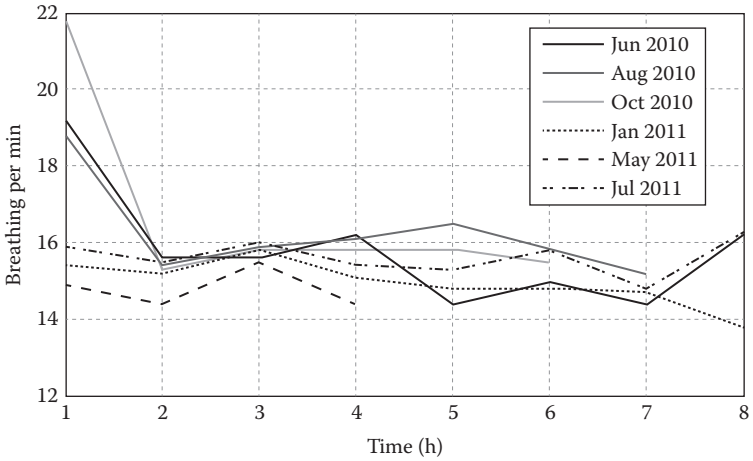

FIGURE 8.18
Respiration frequency dynamics during sleep for one crewmember of MARS-500.

Processing of this experimental data has revealed the individual characteristics of different stages of sleep for the crew members. Some of them have a longer period of falling asleep and more restless sleep, while others, on the contrary, fall asleep faster and have more calm and regular breathing thereafter. Duration of sleep for each subject during the project changed individually, for four out of six crew members, during the first three series of experiments, a greater than 10% decrease in sleep duration was registered. In the second half of the experiment, significant changes in monitored parameters (respiratory rate and the duration of movement artifacts during sleep) did not occur, which indicates a good tolerance of the crew to the conditions of prolonged isolation. Breathing sleep disorders were not detected for any of the crew members.

8.4.2 Noncontact Screening of Sleep Apnea Syndrome Using Bioradiolocation

One of the priority applications of BRL in sleep medicine is detection of sleep disordered breathing (SDB). The objective of a study conducted in 2012 was to estimate the diagnostic ability of BRL for noncontact screening of SDB in adults in comparison with the gold-standard full-night polysomnography (PSG) method.

The seven test subjects included four males and three females, aged 43–62 years, with body mass index or BMI in the range 21.6–57.7. They had a range of severities of obstructive sleep apnea syndrome (OSAS): 4 severe; 1 moderate; 1 mild; 1 normal. The PSG records were collected with an Embla N7000 system in the sleep laboratory of the Almazov Federal Heart, Blood and Endocrinology Centre, while simultaneously monitoring with a BioRASCAN system. Subsequently, PSG records were analyzed by a certified specialist and the verification of corresponding BRL signals was performed manually by a trained operator.

Algorithms applying wavelet transform (WT) and neural network (NN) were previously used for recognition of breathing patterns of BRL signals during noncontact estimation of sleep apnea syndrome (SAS) severity (Alekhin 2013).

The proposed algorithm consists of two main steps. In the first step, WT is applied to extract informative feature. Initially, a general class of wavelets is defined, then a set of wavelet bases with ordinal indexes for wavelet families from the general class is formed,

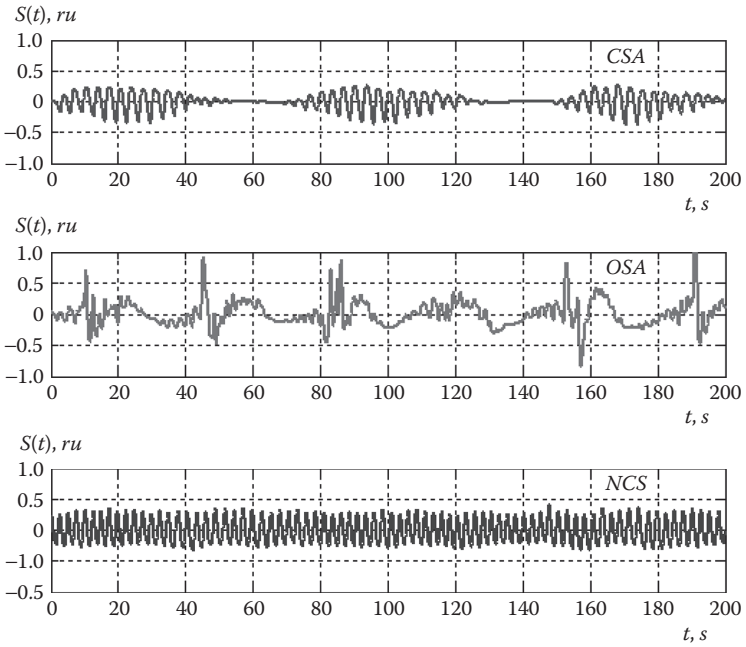

FIGURE 8.19
Bioradiolocation signals for the recognition of clinically verified breathing patterns of BRL signals corresponding to the following syndromes: obstructive sleep apnea (OSA); central sleep apnea (CSA); and normal calm sleeping (NCS) without SDB.

and then the optimal level of wavelet decomposition is determined. In the second step after preliminary estimation of number of NNW hidden layers, the best NNW learning algorithm is applied.

This proposed approach was tested for recognition of clinically verified breathing patterns of BRL signals corresponding to the following syndromes: obstructive sleep apnea (OSA); central sleep apnea (CSA); normal calm sleeping (NCS) without SDB Figure 8.19.

The analysis of PSG records revealed in total 2700 episodes of SDB: 1279 incidents of OSA; 106 of CSA; 495 for mixed sleep apnea (MSA); and 820 hypopneas (HYPA). The result of verification of BRL signal patterns for SDB in comparison with PSG was as follows: 1955 true positives; 745 false positives; 868 false negatives. Thus, BioRASCAN system displayed a sensitivity of 69 % and an accuracy of 72 % in noncontact screening for SDB. These results should be considered clinically significant since, in each case, the estimate of apnea–hypopnea index (AHI) for the BRL method overlaps with the same range for the OSAS severity scale using the PSG method.

8.4.3 Human *Physiological Psycho-Emotional State Monitoring* and *Professional Testing*

Another possible area of BRL application is monitoring of the human psycho-emotional state. At BMSTU, we investigated this in experiments involving an internal stress factor. An example of a recorded BRL signal for this kind of test is given in Figure 8.20 for a ringing mobile phone as a stress factor. Note that while the phone was ringing, the amplitude of chest movements caused by breathing became two times lower than without the ringing.

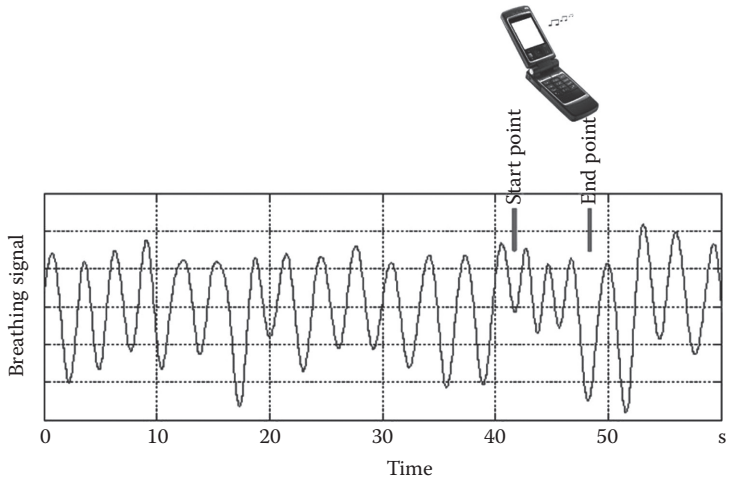

FIGURE 8.20
Received bioradar signal for the additional stress factor experiment. The ringing mobile telephone produces a distinct change in the respiration signal.

As for breathing frequency, its value slightly increased. That is, when the phone rings, the subjects breathing becomes shallow and rapid.

To imitate a stress factor with a longer duration, the standard mental load test was used. During the 5-minute test, the examinee was asked to solve simple mathematical problems. The test sample included 52 subjects (25 males and 27 females, aged 19–21 years). In this case, respiration and heart beat frequency parameters remained almost the same, but their variability did not. A histogram for vital sign frequencies monitored by BRL may be used as a convenient way to represent changes caused by mental load. Histograms of the heart beat intervals before and after the testing for one of the examinees are shown in the Figure 8.21. During mental loading, heart rate increased from 1.2 to 1.5 Hz, and pulse interval variability decreased (standard deviation went from 0.25 to 0.06 sec).

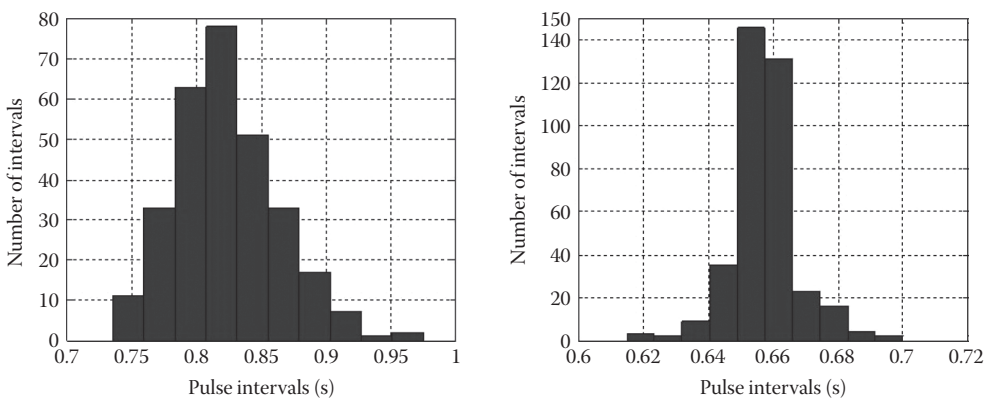

FIGURE 8.21
Histograms of heart beat intervals before and after the standard mental test for one of the examinees.

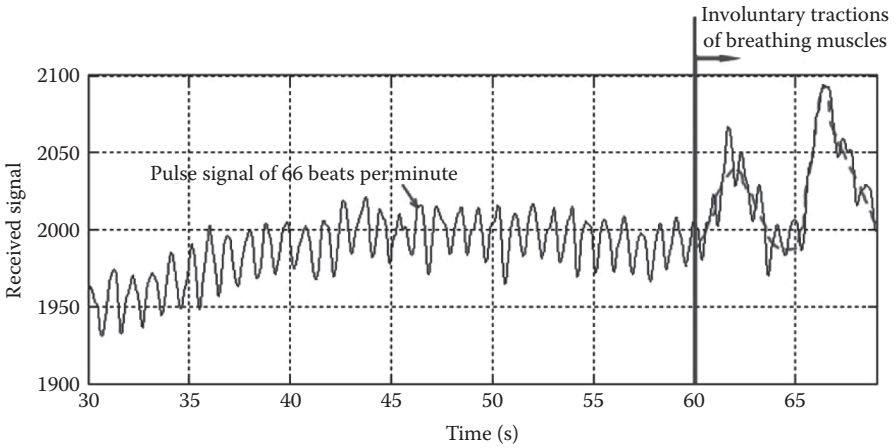

FIGURE 8.22
Received BRL signal for a breath-holding test.

The experimental data analysis showed that performing mental loading leads to a statistically significant change in heart rate (a confidence level of $p = 0.80$), but the changes in respiratory rate were not statistically significant.

The BRL method can be used during the widely known Shtange's and Hench's breath holding tests for estimating cardiorespiratory fitness. These are used in the selection of pilots, submariners, and divers. An example of a recorded bioradar signal for this kind of test is presented in Figure 8.22. After holding the breath for 1 minute , involuntary contraction of respiratory muscles took place because of oxygen starvation. However, examinee continued holding his breath even after this phenomenon. The problem is that the correct duration of this test for the examinee should be estimated without the period when such involuntary contraction occurs as shown on the right side of Figure 8.22. Thus, it was proved that usage of BRL in this type of test would sufficiently improve its accuracy.

8.4.4 Estimation of Small Laboratory Animal Activity by Means of Bioradar

BRL can measure both humans and animals for pharmacology and zoo-psychology studies for developing new medicines or conducting behavioral tests (Kropveld 1993, Anishchenko 2009).

Currently tests of drugs and toxic substances use invasive methods to measure variations in physiological parameters of laboratory animals. The researcher in this case subjectively estimates the animal's locomotor activity visually and has no definitive measure of activity. It is possible to reduce the workload on the researcher by applying automated methods to estimate locomotor activity using specially designed video-tracking systems. The main drawback of this is that it cannot be used for animals in optically opaque mazes.

There are devices based on different physical principles, which can be used for automated monitoring of motor activity parameters of laboratory animals. Some of them use pressure sensors mounted in the cage floor, which allows estimation of the animal movement in the cage (Bederman 1972). Others use light sources and optical sensors integrated in the cage walls (Hideo 1997). Also, for similar purposes, electromagnetic radiation has been proposed (Salmons 1969).

The main drawback of all these devices is the manufacturing complexity of the cage in which the animal is placed during the experiment. Furthermore, these cages are designed

for a certain type of laboratory animal for which specific morphometric features need to be considered. That is why, generally, the locomotor activity of the animals is visually estimated by a researcher.

Devices based on the method of BRL are free from the drawbacks listed above. They measure a phase shift of the radar signal reflected from the biological subject, which is caused by body surface displacements. This method does not require design and construction of special cages, and may be used with the plastic containers in which animals are usually kept, or in optically opaque (but electromagnetically transparent) mazes. Another advantage of bioradar sensors in solving the above problems is the possibility of direct automated evaluation of the animals' activity for prolonged periods, as proven by the experiments conducted at BMSTU in 2009. A sketch and photo of the experimental set up are given in Figure 8.23.a and 23.b, respectively. During the experiments, the animal (a four-month-old Wistar rat) was placed into a box of 70×70×70 cm size with dielectric walls. Transmitting and receiving antennas of the radar were directed into the box as shown in Figure 8.23.b.

The signal reflected from the animal was recorded for further processing. The distance between the antenna block and carton was approximately 1 m. This short distance was necessary due to the relatively small scattering cross section of the animal. The video signal was also recorded using a simple web camera placed over the box. Behavior and movement activity of the animal during the experiment, as recorded by the camera, was used for the identification of different types of a rat locomotor activity in the BRL signals. It is known that power flux density near radar-receiving antennas declines inversely with the fourth power of the range between antennas and an object, making the power of the reflected signal greatly dependent on the distance between the antenna block and animal. Because of this, an accurate estimation of the rat's movement is challenging. A corner reflector was used to make the power of the reflected signal indifferent to the location of the animal inside the box. It was formed by covering two walls and the floor of the box with metallic film.

Figure 8.24 presents a fragment of the BRL signal in which intervals of inactivity and activity may be easily distinguished by reflected signal amplitude.

If the intensity of the animal's movement activity, as well as different types of activity, needs to be determined, then spectral analysis can be used. Figure 8.25 presents the spectra for BRL signals corresponding to different states or activities of the animal.

The spectra differ greatly in both magnitude and form. Thus, it is possible to distinguish grooming from steady state, sleep, or active movements of the animal using spectral analysis of BRL signals.

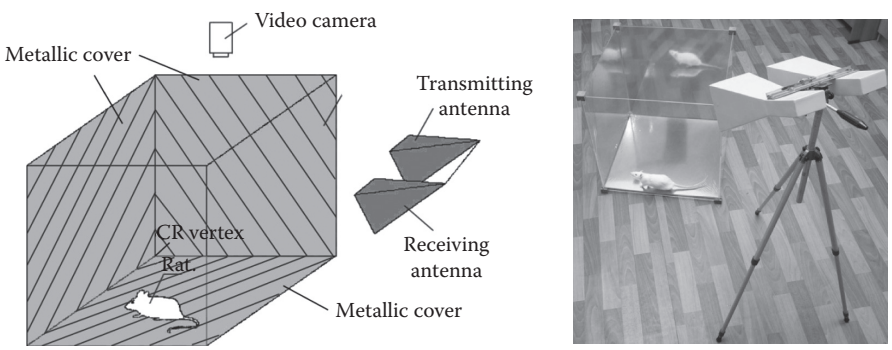

FIGURE 8.23
Schematic and photo of the animal activity experiment set up.

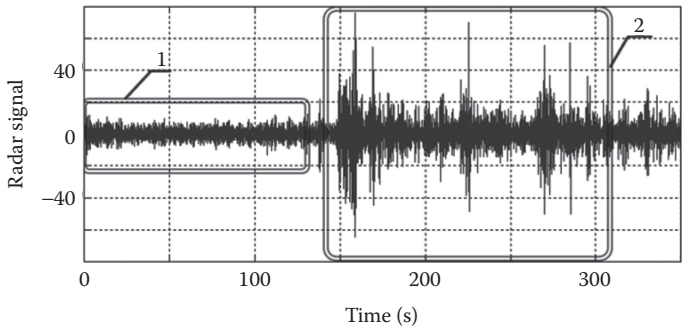

FIGURE 8.24
Radar signal reflected from an animal (1 – steady state, 2 – physical activity).

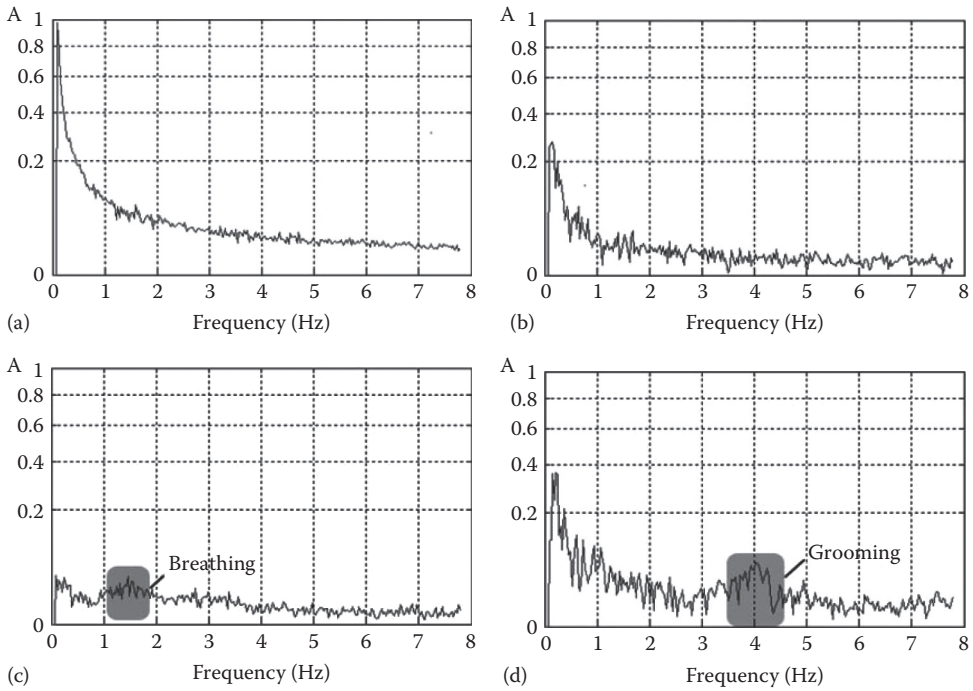

FIGURE 8.25
The results of the animal activity experiments showing the distinct spectra of different activities: (a) Active movements. (b) Steady state. (c) Sleeping. (d) Grooming.

8.5 Conclusion

This chapter presented the BRL method for remotely monitoring human vital signs and animal activities. It discussed the technical characteristics of the bioradar system created at the Remote Sensing Laboratory of Bauman Moscow State Technical University and the results of experiments using variants of this system. In experiments where bioradar was used simultaneously with standard (contact) methods and video for

monitoring respiratory and heart rate parameters, the BRL performed as reliably and effectively, which makes accurate remote noncontact monitoring possible. One set of experiments showed how the BRL is suitable for remote measurement and estimation of human psycho-emotional state. The remote measurements showed the adaptive capabilities of the organism (including tolerance to oxygen starvation) during cardiorespiratory fitness testing. Moreover, BRL can measure and estimate sleep quality and apnea syndrome severity, where it showed a good agreement with gold-standard full night PSG testing.

BRL is a relatively new technology, which now is making its first attempts to enter the remote medical monitoring technology field. Experiments show that it has tremendous possibilities for this.

Editor's note

The American Food and Drug Administration (FDA) had approved at least one UWB radar for remote patient monitoring. The SensioTec™ Virtual Medical Assistant® (VMA) uses a UWB radar and motion sensors built into a pad which can fit under a hospital bed mattress. The VMA connects to a network of wireless connections to present patient data at remote locations (http://sensiotec.com).

References

Alekhin, M., Anishchenko L., Tataraidze A. et al. 2013. "Selection of Wavelet Transform and Neural Network Parameters for Classification of Breathing Patterns of Bio-radiolocation Signals" *Biomedical Informatics and Technology*, T.D. Pham et al. (Eds.): ACBIT 2013, CCIS 404, pp. 175–178. Springer, Heidelberg (2013). http://link.springer.com/chapter/10.1007/978-3-642-54121-6_15

Alekhin, M., Anishchenko, L., Tataraidze, A. et al. 2013. "Comparison of Bioradiolocation and Respiratory Plethysmography Signals in Time and Frequency Domains on the Base of Cross-Correlation and Spectral Analysis," *International Journal of Antennas and Propagation*, 6 pages.3

Anishchenko, L.N. and Parashin V. B. 2008. "Design and application of the method for biolocation data processing," *Proceedings of the 4th Russian-Bavarian Conference on Biomedical Engineering at Moscow Institute of Electronic Technology (Technical University)*, pp. 289–294.

Anishchenko, L.N., Bugaev, A.S., Ivashov, S.I., et al. 2009. "Application of Bioradiolocation for Estimation of the Laboratory Animals' Movement Activity," *PIERS Online*, 5(6), 551–554.

Bederman, S., Lankford L. 1972. *Apparatus for measuring the activity of laboratory animals*, US Pattent 3633011.

Bimpas, M., Paraskevopoulos, N., Nikellis, K., et al. 2004. "Development of a three band radar system for detecting trapped alive humans under building ruins," *Progress In Electromagnetic Research*, PIER 49, 161–188.

Boric-Lubecke, O., Lin, J., Park, B-K., et al. 2008. "Battlefield triage life signs detection technique," Proc. SPIE Defence and Security Symposium, Vol. 6947 - Radar Sensor Technology XII, No. 69470J, 10 pages.

Bugaev, A.S., Chapursky, V.V., Ivashov, S.I., et al. 2004. "Through Wall Sensing of Human Breathing and Heart Beating by Monochromatic Radar," *Proceedings of the Tenth International Conference on Ground Penetrating Radar, GPR'2004*, Delft, The Netherlands, Vol. 1, 291–294.

Bugaev, A.S., Chapursky, V.V. and Ivashov, S.I. 2005. "Mathematical Simulation of Remote detection of Human Breathing and Heartbeat by Multifrequency Radar on the Background of Local Objects Reflections," *Proc. IEEE International Radar Conference Record*, Arlington, Virginia, USA, 6 pages.

Chen, K.M., Misra, D., Wang, H., et al. 1986. "An X-band microwave life-detection system," *IEEE Trans Biomed Eng 33, 697–702.*

Chen, K.M., Huang, Y., Shang, J. et al. 2000. "Microwave Life Detection Systems for Searching Human Subjects Under Earthquake Rubble or Behind Barrier," *IEEE Trans. Biomed. Eng.*, 27(1), 105–114.

Droitcour, A. D., Seto, T. B., Park, B. K. et al. 2009. "Non-contact respiratory rate measurement validation for hospitalized patients," *Proc. of Annual International Conference IEEE Engineering in Medicine and Biology Society*, 4812–4815.

Droitcour, A., Lubecke, V., Lin, J., Boric-Lubecke, O. 2001. "A Microwave Radio for Doppler Radar Sensing of Vital Signs," *Proc IEEE MTT-S Int. Microw. Symp.*, 175–178.

D'Urso, M., Leone, G. and Soldovieri, F. 2009. "A simple strategy for life signs detection via an X-band experimental set-up," *Progress in Electromagnetics Research* C, vol. 9, 119–129.

Greneker, E.F. 1997. "Radar Sensing of Heartbeat and Respiration at a Distance with Applications of the Technology," *Proc. IEE RADAR-97*, 150–153.

Hideo M. 1997. *Method and apparatus for measuring motion amount of laboratory animal*, US Pattent 5608209.

Holzrichter, J. F., Burnett, G. C., Ng, L.C. et al. 1998. "Speech Articulator Measurements Using Low Power EM-Wave Sensors," *J. Acoust. Soc. Am.*, 103(1), 622–625.

Immoreev, I.Y. 2010. "Practical Applications of UWB Technology," *IEEE Aerospace and Electronic Systems Magazine,* 25(2), 36–42.

Ivashov, S.I., Razevig, V.V., Sheyko, A.P. et al. 2004. "Detection of Human Breathing and Heartbeat by Remote Radar," *Progress in Electromagnetics Research Symposium (PIERS 2004)*, Pisa, Italy, 663–666.

Kelly, J.M., Strecker, R.E. and Bianchi, M.T. 2012. "Recent Developments in Home Sleep-Monitoring Devices," *ISRN Neurology*, Vol. 2012, Article ID 768794, 10 pages.

Konno K, and Mead J. 1967. "Measurement of the separate volume changes of rib cage and abdomen during breathing," *J. Appl Physiol* 22: 407–422.

Kropveld, D. and Chamuleau, R. 1993. "Doppler radar devise as a useful tool to quantify the liveliness of the experimental animal," Med. & Biol Eng. & *Comput*. 31, 340–342.

Li, C and Lin, J. 2014. "Microwave noncontact motion sensing and analysis," Wiley, New Jersey, 157–185.

Li, J., Liu, L., Zeng, Z. et al. 2012. "Simulation and signal processing of UWB radar for human detection in complex environment," *Proc. of 14th Ground Penetrating Radar (GPR) Conference*, 209–213.

Liu, L., Liu, Z. and Barrowes, B. 2012. "Through-wall bio-radiolocation with UWB impulse radar: observation, simulation and signal extraction," *IEEE Journal on Selected Topics in Applied Earth Observations and Remote Sensing*, vol. 4, no. 4, 791–798.

Massagram, W., Lubecke, V. M., and Boric-Lubecke, O. 2011. "Feasibility assessment of Doppler radar long-term physiological measurements," *Proc. of Annual International Conference IEEE Engineering in Medicine and Biology Society*, 1544–1547.

Otsu, M., Nakamura, R. and, Kajiwara, A. 2011. "Remote respiration monitoring sensor using stepped-FM," *Sensors Applications Symposium (SAS), 2011 IEEE*, 155–158.

Rechtschaffen, A. and Kales, A. 1968. *A Manual of Standardized Terminology: Techniques and Scoring System for Sleep Stages of Human Subjects*. Los Angeles: UCLA Brain Information Service/Brain Research Institute.

Salmons, T. 1969. *Activity detector,* US Patent 3439358.

Soldovieri, F., Catapano, I., Crocco, L. et.al. 2012. "A Feasibility Study for Life Signs Monitoring via a Continuous-Wave Radar," *International Journal of Antennas and Propagation*, vol. 2012, Article ID 420178, 5 pages.

Staderini, E.M. 2002. "UWB Radars in Medicine," *IEEE AESS Systems Magazine*, 17, 13–18.

Vasu, V., Heneghan, C., Sezer, S. et. al. 2011. "Contact-free Estimation of Respiration Rates during Sleep," *Proc. of 22nd IET Irish Signals and Systems Conference*.

Wang, F-K., Horng, S-H., Peng, K.C. et.al. 2013. "Detection of Concealed Individuals Based on Their Vital Signs by Using a See-Through-Wall Imaging System With a Self-Injection-Locked Radar," *Microwave Theory and Techniques, IEEE Transactions on* , vol.61, no.1, 696–704.